XLVI CILAMCE
VITÓRIA - ES - BRAZIL - 2025
XLVI IBERO-LATIN AMERICAN CONGRESS ON COMPUTIONAL METHODS IN ENGENEERING

High-order boundary conditions for the lattice-Boltzmann simulation of isothermal fluid flow

Matheus A. Iurk[1], Luiz A. Hegele Junior[2], Paulo C. Philippi[1]

[1]*Mechanical Engineering Graduate Program, Pontifical Catholic University of Parana, Brazil*
R. Imac. Conceição, 1155 - Prado Velho, Curitiba - PR, 80215-901
matheusamplatz@gmail.com, paulo.philippi@pucpr.br
[2]*Department of Petroleum Engineering, Santa Catarina State University*
Balneário Camboriú, SC, 88336-275
luiz.hegele@udesc.br,

Abstract. Dealing with boundary conditions (BC) was ever considered a puzzling question in the Lattice Boltzmann (LB) method. The most popular BC models are based on Ad-Hoc rules and, although these BC models were shown to be suitable for low-order LB equations, their extension to high-order LB was shown to be a very difficult problem and, at the author's knowledge, never solved with satisfaction. The main question to be solved is how to deal with a problem when the number of unknowns (the particle populations coming from the outside part of the numerical domain) is greater than the number of equations at our disposal at each boundary site. Recently, BC models based on the regularization of the LB equation or, moment-based models were proposed. These moments replace the discrete populations as unknowns, independently of the number of discrete velocities that are needed to solve a given problem. In this work, we search for a unique and general moment-based method to solve the BC problem. The method is applied to investigate the problem of incompressible flow development inside a 2D channel in conjunction with the use of a third-order LB scheme.

Keywords: fluid mechanics, high-order lattice-Boltzmann, boundary conditions.

1 Introduction

One of the key issues in a numerical method is the application of boundary conditions. While solving the core flow itself is the main goal of every numerical method, the way boundary conditions —- either Dirichlet, Neumann, or Robin — are specified is usually considered a less important problem. Nevertheless, it has been shown by Hegele et al. [1] and Bazarin et al. [2], that a careful approach for the fluid-solid interaction might lead to a significant improvement of the description of the flow and the numerical stability of the method itself.

A lot of effort has been devoted to the boundary conditions for the lattice Boltzmann framework, but the most recent thorough comparison of different models for boundary conditions was published a decade ago by Latt et al. [3] and Luo et al. [4]. In this work, only Dirichlet boundary conditions will be considered.

Hollis et al. [5] use mass conservation with a finite-difference scheme to determine second-order moments. To get a determined system, some particle distributions are desconsidered, and only the non-equilibrium parts are retained of selected distributions to perform the reconstruction. Latt et al. [3] exploit the symmetry of second-order moments to recover unknown distributions, following Zou and He [6]. Verschaeve [7] adds the relation between second-order moments and the strain rate tensor, together with the mass conservation condition for incompressible flows. Malaspinas et al. [8] formulate an overdetermined system based on density, first and second-order moments, solved throught minimization. Finally, Mohammed and Reis [9] select linearly independent equations for hydrodynamic moments to reconstruct the distributions.

Seeking a unique and general method for solving the boundary conditions, avoiding the appeal to *ad hoc* rules, we extend the moment-based method for boundary conditions to high-order lattice Boltzmann schemes. The flow development inside a 2D channel in conjunction with the use of a third-order LB scheme is considered here as a sample case.

2 Theoretical background

2.1 The LB equation

Let D be the Euclidean dimension of the physical space. The distribution $f\ (\mathbf{x}, \xi, t)$, solution of the Boltzmann equation

$$\partial_t f + \xi \cdot \nabla f = \Omega \tag{1}$$

may be considered, for each $\mathbf{x}, t$ as a map from the continuous velocity space ξ^D onto the space $\mathcal{R}$ of real numbers. In fact, it belongs to the Hilbert space $\mathcal{H}$ of square integrable functions $f : \xi^D \to \mathcal{R}$ and may be written in terms of an orthogonal basis of $\mathcal{H}$ that will be, here, considered as the infinite set of Hermite polynomial tensors.

The collision term Ω in eq. (1), is usually written as a Bhatnagar, Gross and Krook (BGK) relaxation term, as proposed by Bhatnagar et al. [10]. In dimensionless form

$$\overline{\Omega} = -\frac{\overline{f} - \overline{f}^{eq}}{\tau^*},$$

where τ^* is a dimensionless relaxation time, $\tau^* = \tau/\delta$, δ is the time step, and the Maxwell–Boltzmann equilibrium distribution can be written, in its dimensionless form, as

$$\overline{f}^{eq} = \frac{1}{(2\pi)^{\frac{D}{2}}} \rho^* e^{-\frac{(\xi_0 - \mathbf{u}_0)^2}{2}},$$

where $\rho^* = n/n_0$ and $\mathbf{u}_0\ (\mathbf{x}, t)$ is the local macroscopic velocity in point $\mathbf{x}$ and at time t.

In its dimensionless discrete form, eq. (1) can be written as

$$\partial_{t^*} \overline{f}_i + \mathbf{e}_i \cdot \nabla \overline{f}_i = -\frac{\overline{f}_i - \overline{f}_i^{eq}}{\tau^*}, \tag{2}$$

where $\overline{f}_i = \overline{f}_i\ (\mathbf{x}, \xi_i, t)$, $i = 0, ..., b-1$, are the populations of particles that, at time t, have a velocity ξ_i in site $\mathbf{x}$, $t^* = t/\delta$, $\nabla^* = \nabla/h$, and h is the orthogonal distance between two contiguous sites.

Using a first order Taylor expansion for $\overline{f}_i\ (\mathbf{x} + \mathbf{e}_i h, t + \delta)$, and after some algebraic manipulation, the LB algorithm becomes

$$\overline{f}_i\ (\mathbf{x} + \mathbf{e}_i h, t + \delta) = \frac{1}{\tau^*} \overline{f}_i^{eq}\ (\mathbf{x}, t) + \left(1 - \frac{1}{\tau^*}\right) \overline{f}_i + O\left(h^2\right). \tag{3}$$

The LB algorithm described by eq. (3) is suitable for population-based models and involves two main steps: collision and propagation. The right-hand side of eq. (3) represents the collision step, while the left-hand side corresponds to propagation.

2.2 Third-order moments-based LB models

In its discrete form the population of particles $\overline{f}_i$ can be written for a third-order LB model as

$$\overline{f}_i = W_i \begin{pmatrix} a^{(0)} H^{(0)} + \left(a_x^{(1)} H_x^{(1)} + a_y^{(1)} H_y^{(1)}\right) + \\ + \frac{1}{2}\left(a_{xx}^{(2)} H_{xx}^{(2)} + 2a_{xy}^{(2)} H_{xy}^{(2)} + a_{yy}^{(2)} H_{yy}^{(2)}\right) + \\ + \frac{1}{6}\left(a_{xxx}^{(3)} H_{xxx}^{(3)} + 3a_{xxy}^{(3)} H_{xxy}^{(3)} + 3a_{xyy}^{(3)} H_{xyy}^{(3)} + a_{yyy}^{(3)} H_{yyy}^{(3)}\right) \end{pmatrix}. \tag{4}$$

Table 1 presents the set of Hermite polynomial tensors, the equilibrium and non-equilibrium Hermitian moments up to the third-order.

When considering $\overline{f}_i$ as a sum of its equilibrium and non-equilibrium parts $\overline{f}_i = \overline{f}_i^{eq} + \overline{f}_i^{neq}$, the Hermitian moments can be also written as a sum of their equilibrium and nonequilibrium parts,

$$a^{(\theta)} = a_{eq}^{(\theta)} + a_{neq}^{(\theta)}.$$

The high-order Hermitian non-equilibrium moment $a_{\alpha\beta\gamma}^{(3)}$ deserves some detailing. The dyadic product $e_{i\alpha} e_{i\beta} e_{i\gamma}$ an be written as

Table 1. Hermite Polynomials and equilibrium and non-equilibrium Hermitian moments up to the third-order.

Order	Hermite polynomial	Equilibrium moments	Non-equilibrium moments
0	1	ρ^*	0
1	$a_s e_{i,\alpha}$	$a_s \rho^* u^*_\alpha$	0
2	$a_s^2 e_{i,\alpha} e_{i,\beta} - \delta_{\alpha\beta}$	$a_s^2 \rho^* u^*_\alpha u^*_\beta$	$a_s^2 \tau^*_{\alpha\beta}$
3	$a_s^3 e_{i\alpha} e_{i\beta} e_{i\gamma} - a_s \left(e_{i\alpha}\delta_{\beta\gamma} + e_{i\beta}\delta_{\alpha\gamma} + e_{i\gamma}\delta_{\alpha\beta}\right)$	$a_s^3 \rho^* u^*_\alpha u^*_\beta u^*_\gamma$	$a_s^3 \left(\widetilde{\pi}^{(3)}_{\alpha\beta\gamma} + u^*_\alpha \tau^*_{\beta\gamma} + u^*_\beta \tau^*_{\alpha\gamma} + u^*_\gamma \tau^*_{\alpha\beta}\right)$

$$
\begin{aligned}
e_{i\alpha}e_{i\beta}e_{i\gamma} \;=\; & \left(e_{i\alpha} - u^*_\alpha\right)\left(e_{i\beta} - u^*_\beta\right)\left(e_{i\gamma} - u^*_\gamma\right) \\
& + \left(e_{i\alpha} - u^*_\alpha\right) u^*_\beta u^*_\gamma + \left(e_{i\beta} - u^*_\beta\right) u^*_\alpha u^*_\gamma + \left(e_{i\gamma} - u^*_\gamma\right) u^*_\alpha u^*_\beta \\
& + u^*_\alpha \left(e_{i\beta} - u^*_\beta\right)\left(e_{i\gamma} - u^*_\gamma\right) + u^*_\beta \left(e_{i\alpha} - u^*_\alpha\right)\left(e_{i\gamma} - u^*_\gamma\right) \\
& + u^*_\gamma \left(e_{i\alpha} - u^*_\alpha\right)\left(e_{i\beta} - u^*_\beta\right) + u^*_\alpha u^*_\beta u^*_\gamma,
\end{aligned}
$$

in such a way that,

$$
\sum_i a_s^3 e_{i\alpha}e_{i\beta}e_{i\gamma}\overline{f}_i^{eq} = a_s^3 \rho^* u^*_\alpha u^*_\beta u^*_\gamma,
$$

and

$$
\sum_i a_s^3 e_{i\alpha}e_{i\beta}e_{i\gamma}\overline{f}_i^{neq} = a_s^3 \left(\widetilde{\pi}^{(3)}_{\alpha\beta\gamma} + \overline{\pi}^{(3)}_{\alpha\beta\gamma}\right),
$$

where $\widetilde{\pi}^{(3)}_{\alpha\beta\gamma}$ is a third-order *diffusive* component

$$
\widetilde{\pi}^{(3)}_{\alpha\beta\gamma} = \sum_i \left(e_{i\alpha} - u^*_\alpha\right)\left(e_{i\beta} - u^*_\beta\right)\left(e_{i\gamma} - u^*_\gamma\right)\overline{f}_i^{neq}.
$$

and

$$
\overline{\pi}^{(3)}_{\alpha\beta\gamma} = u^*_\alpha \tau^*_{\beta\gamma} + u^*_\beta \tau^*_{\alpha\gamma} + u^*_\gamma \tau^*_{\alpha\beta}.
$$

is an *advective* component dependent on the lower second-order nonequilibrium moments $\tau^*_{\alpha\beta}$.

When dealing with a single-component system of particles, the hightest order non-equilibrium moment is the heat flow

$$
q_\alpha = \frac{1}{2}\sum_i \left(e_{i\alpha} - u^*_\alpha\right)\left(e_{i\beta} - u^*_\beta\right)^2 \overline{f}_i^{neq},
$$

and this non-equilibrium moment can be expressed in terms of Hermitian moments as Mattila et al. [11].

$$
q_\alpha = \frac{1}{2} a_s^3 \left(a^{(3)}_{neq,\alpha\beta\beta} - \left(u^*_\alpha \tau^*_{\beta\beta} + 2u^*_\beta \tau^*_{\alpha\beta}\right)\right).
$$

The diffusive part is a representation of a moment in a moving frame of reference, while the advective part accounts for the bulk flow contribution. We therefore have an opportunity to acknowledge the essential role of advective transport in high Re flows. Namely, instead of completely filtering the high-order non-equilibrium moments, like in the original regularization procedure, the idea is to filter only the diffusive parts; the aim is to retain the advective parts to the fullest extent possible with the adopted decomposition.

Therefore by filtering all the third-order diffusive parts, we obtain for isothermal flows

$$
a^{(3)}_{neq,\alpha\beta\gamma} = a_s^3 \left(u^*_\alpha \tau^*_{\beta\gamma} + u^*_\beta \tau^*_{\alpha\gamma} + u^*_\gamma \tau^*_{\alpha\beta}\right), \tag{5}
$$

related to the advection transport of the viscous stress tensor components.

The expression in eq. (5) was derived by Malaspinas [12] and Mattila et al. [11] using different approaches and showed improved stability ranges. This appears to verify that the *rationale* behind filtering only the diffusive parts, and thus retaining the advective parts, is both reasonable and useful as a guiding principle when constructing stable LB schemes.

3 The simulation algorithm for isothermal systems

Table 2 shows the Hermitian moments to be used in the expansion given by eq. (4) in isothermal problems.

Table 2. Hermitian moments

Order	Hermitian moments for isothermal flow
$a^{(0)}$	ρ^*
$a_\alpha^{(1)}$	$a_s\rho^* u_\alpha^*$
$a_{\alpha\beta}^{(2)}$	$a_s^2\left(\rho^* u_\alpha^* u_\beta^* + \tau_{\alpha\beta}^*\right)$
$a_{\alpha\beta\gamma}^{(3)}$	$a_s^3\left(\rho^* u_\alpha^* u_\beta^* u_\gamma^* + u_\alpha^*\tau_{\beta\gamma}^* + u_\beta^*\tau_{\alpha\gamma}^* + u_\gamma^*\tau_{\alpha\beta}^*\right)$

After the streaming step, all populations $\overline{f}_i(\mathbf{x},t)$ are known for each node $\mathbf{x}$ and time t. We can then calculate the dimensionless density and local velocity, respectively, through

$$\rho^* = \textstyle\sum_i \overline{f}_i \quad u_\alpha^* = \frac{1}{\rho^*}\sum_i \overline{f}_i e_{i\alpha},$$

and the equilibrium populations $\overline{f}_i^{eq}(\rho^*, \rho^* u_\alpha^*)$ using eq. (4) with the equilibrium moments up to the third-order as shown in Table 1, and the viscous stress tensor

$$\tau_{\alpha\beta}^* = \sum_i \left(\overline{f}_i - \overline{f}_i^{eq}\right) e_{i\alpha} e_{i\beta}$$

The values of ρ^*, u_α^*, and $\tau_{\alpha\beta}^*$ are then used to reconstruct the pre-collisional populations using eq. (4) with the moments shown in Table 2.

4 High-order moments based boundary conditions

Various approaches can be used to define boundary conditions in the LBM. In this work, the moment-based condition was used.

Consider Fig. 1 representing a channel with dimensions L_x and L_y with $N_y = \frac{L_y}{h}+1$ nodes and $N_x = \frac{L_x}{h}+1$ nodes along the y and x coordinates, respectively. The figure also shows the D2V17 set of discrete lattice vectors $\mathbf{e}_i$ $i = 0, ..., 16$ for a node at the first (a), second (b) and third (c) columns at the entrance of the channel.

Increasing the order of the LB algorithm means that we are increasing the order of approximation to the continuous Boltzmann equation (eq. (1)) for which we are required to increase the spatial resolution. In this sense, the channel entrance in Fig. 1 is represented by three columns of nodes instead of a single one as would be the case for second-order LB algorithms.

All the particle populations represented in red came from outside of the numerical domain and are unknown.

For the first column in Fig. 1.a we consider $I_1 = \{0, 2, 3, 4, 6, 7, 10, 11, 14, 15, 16\}$ as the set of incoming directions from the fluid nodes, located inside the numerical domain. The particle populations along these directions are known and represent the information from fluid flow that arrives at the boundary node along the characteristic lines (the lattice directions).

Set I_2 for the nodes at the second column (Fig. 1.b) is given by $I_2 = \{0, 1, 2, 3, 4, 5, 6, 7, 8, 10, 11, 14, 15, 16\}$ and set I_3 at the third column (Fig. 1.c) is given by $I_3 = \{0, 1, 2, 3, 4, 5, 6, 7, 8, 9, 10, 11, 12, 14, 15, 16\}$.

Therefore all the populations of particles $\bar{f}_i$, $i \in I$, are known, whereas the populations $\bar{f}_i$, $i \notin I$, are unknowns at the boundary nodes. In the moments-based approach, these unknown populations are written following eq. (4) and so the problem of finding their values is reduced in 2D to the problem of finding the values of the Hermitian moments ($a^{(0)}$, $a_x^{(1)}$, $a_y^{(1)}$, $a_{xx}^{(2)}$, $a_{xy}^{(2)}$, $a_{yy}^{(2)}$, $a_{xxx}^{(3)}$, $a_{xxy}^{(3)}$, $a_{xyy}^{(3)}$, $a_{yyy}^{(3)}$), by solving the following linear system of equations,

$$\sum_{i\in I} \overline{f}_i H^{(0)} + \sum_{i\notin I} \hat{\overline{f}}_i H^{(0)} = a^{(0)}, \tag{6}$$

$$\sum_{i\in I} \overline{f}_i H_\alpha^{(1)}(a_s e_i) + \sum_{i\notin I} \hat{\overline{f}}_i H_\alpha^{(1)}(a_s e_i) = a_\alpha^{(1)}, \tag{7}$$

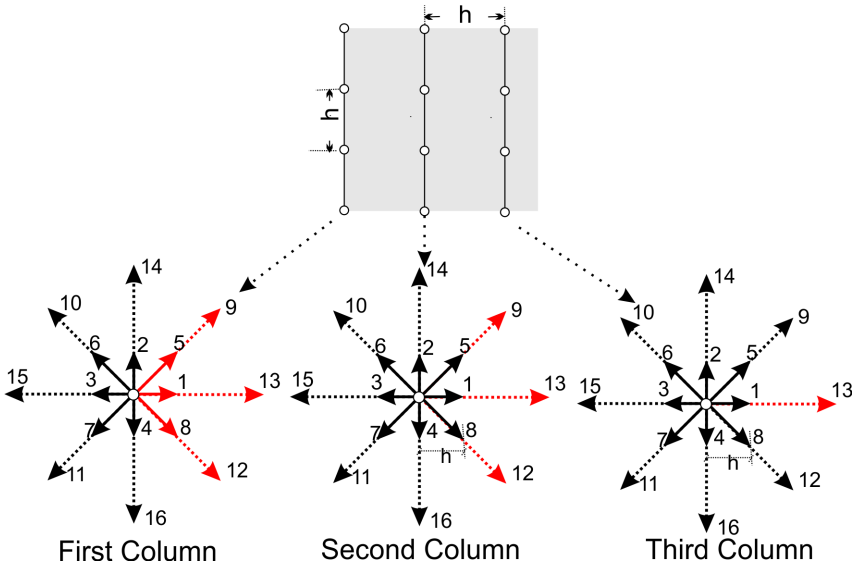


Figure 1. Boundary nodes for the D2V17 LBE. Particle populations in red came from outside the numerical domain and are unknown.

$$\sum_{i\in I} \overline{f}_i H^{(2)}_{\alpha\beta}\left(a_s e_i\right) + \sum_{i\notin I} \hat{\overline{f}}_i H^{(2)}_{\alpha\beta}\left(a_s e_i\right) = a^{(2)}_{\alpha\beta}, \tag{8}$$

$$\sum_{i\in I} \overline{f}_i H^{(3)}_{\alpha\beta\gamma}\left(a_s e_i\right) + \sum_{i\notin I} \hat{\overline{f}}_i H^{(3)}_{\alpha\beta\gamma}\left(a_s e_i\right) = a^{(3)}_{\alpha\beta\gamma}. \tag{9}$$

In the above system, we used the symbol $\hat{\overline{f}}_i$ to designate the unknown populations, for which $i \notin I$, and that will be given in terms of their moments, following eq. (4).

5 A sample case: flow development inside a 2D channel

We restrict this analysis to pressure-driven flows although the method can be easily extended to other boundary conditions.

In the first colum of nodes, we can consider that at the first column of nodes, $\rho^* = known$, $u^*_y = 0$ and $\frac{\partial u^*_y}{\partial y^*} = 0$. As a consequence, $\tau^*_{xx} = \tau^*_{yy} = 0$.

Furthermore, supposing the flow to be incompressible leads to $\frac{\partial u^*_x}{\partial x^*} = 0$.

From Table 2 it results that $a^{(1)}_y = a^{(2)}_{yy} = a^{(3)}_{yyy} = a^{(3)}_{xyy} = 0$. Additionaly, $a^{(2)}_{xx} = a^2_s \rho^* \left(u^*_x\right)^2$, $a^{(2)}_{xy} = a^2_s \tau^*_{xy}$, $a^{(3)}_{xxx} = a^3_s \rho^* \left(u^*_x\right)^3$ and $a^{(3)}_{xxy} = a^3_s \left(2u^*_x \tau^*_{xy}\right)$.

Therefore, the only unknowns are u^*_x and τ^*_{xy} that can be obtained by solving

$$\sum_{i\in I} \overline{f}_i H^{(1)}_{x} + \sum_{i\notin I} \hat{\overline{f}}_i H^{(1)}_{x} = a^{(1)}_x = a_s \rho^* u^*_x, \tag{10}$$

$$\sum_{i\in I} \overline{f}_i H^{(2)}_{xy,i} + \sum_{i\notin I} \hat{\overline{f}}_i H^{(2)}_{xy,i} = a^{(2)}_{xy} = a^2_s \tau^*_{xy}. \tag{11}$$

Remark that although the only unknowns are $a^{(1)}_x$ and $a^{(2)}_{xy}$ the populations $\hat{\overline{f}}_i$ in eqs. (10) and (11) are dependent on the third-order Hermitian moments $a^{(3)}_{xxx}$ and $a^{(3)}_{xxy}$. Replacing these moments in terms of u^*_x and τ^*_{xy} will give a non-linear system in the horizontal component of the velocity u^*_x and this is undesirable, specially for the second and third columns of notes at the boundary where both u^*_x and u^*_y are unknowns.

Searching for a general method for solving the linear system given by eqs. (6)-(9) for all the three columns of boundary nodes we propose an interaction method by considering that all the third-order Hermitian moments $a^{(3)}_{\alpha\beta\gamma}$ are known from the previous time step. These moments are initialized as $a^{(3)}_{\alpha\beta\gamma} = 0$ and the iteration proceeds till convergence.

For the second and third column of nodes, the linear system of equations in eqs.(6)-(9) is a closed system of 10 equations with 10 unknowns that can be rearranged in the form

$$A\mathbf{a} = \mathbf{b},$$

where $\mathbf{a} = \left[a^{(0)}, a_x^{(1)}, a_y^{(1)}, a_{xx}^{(2)}, a_{xy}^{(2)}, a_{yy}^{(2)}, a_{xxx}^{(3)}, a_{xxy}^{(3)}, a_{xyy}^{(3)}, a_{yyy}^{(3)}\right]^T$. Nevertheless, matrix A showed to be ill-conditioned.

For solving the system we used the same method we used for the first column of nodes, but now considering $\mathbf{a} = \left[a^{(0)}, a_x^{(1)}, a_y^{(1)}, a_{xx}^{(2)}, a_{xy}^{(2)}, a_{yy}^{(2)}\right]^T$ and vector $\mathbf{b}$ as dependent of the third-order Hermitian moments $a_{xxx}^{(3)}, a_{xxy}^{(3)}, a_{xyy}^{(3)}, a_{yyy}^{(3)}$, supposed to be known from the previous time step and initialized as $a_{\alpha\beta\gamma}^{(3)} = 0$.

6 Numerical results

The incompressible flow in a 2D channel is a benchmark problem commonly used to test numerical algorithms. Compared to 3D problems, it is mathematically and computationally simpler to solve, has a known analytical solution, and exhibits a well-behaved flow pattern. These characteristics make it suitable for analyzing the stability, consistency, and convergence of newly developed numerical methods.

The analytical solution is obtained solving the Navier-Stokes equation with the following considerations: steady state, incompressible and fully developed flow. However, this solution cannot be directly used to compare with the numerical results, so it must be expressed in dimensionless form. After some algebraic manipulation, the dimensionless analytical solution for this case is given by

$$u^* = U^* \left[1 - \left(\frac{y - \frac{N_y - 1}{2}}{\frac{N_y - 1}{2}}\right)^2\right], \tag{12}$$

where U^* is the maximum dimensionless velocity in the center of the channel and N_y is the channel width. With eq. (12) the velocity profile obtained is parabolic.

In addition, the dimensionless pressure gradient is given by

$$\Delta\rho^* = -\frac{4U^*\nu^*\rho^*N_x}{\left(\frac{N_y}{2}\right)^2}. \tag{13}$$

where ν^* is the dimensionless absolute viscosity of the fluid and N_x is the channel length.

Finally, the error was computed by the following equation

$$Error\,(\%) = \sqrt{\frac{\sum_x \left(u_{num} - u_{ana}\right)^2}{\sum_x u_{ana}^2}} \tag{14}$$

The purpose of this section is to present numerical simulations conducted to evaluate the newly proposed approach to solve the system of equations at the boundary. Simulations were performed for the mesh 2752×128.

At the inlet, we considered $\rho^* = 1.0$ and $\Delta\rho = 5 \times 10^{-5}$. At the upper and lower walls, the velocity components were set to zero. All boundaries were modeled with the moment-based condition and adopted the newly proposed approach to solve the system of equations at the boundary.

With a mesh, 2752×128, and a relaxation time of 0.51, the Re achieved was equal to 82 with an error of 1.81%. The development of the velocity profile can be seen in the Fig. 2.

7 Conclusions

The use of high-order LB schemes and high-order boundary models can enhance both the stability and accuracy of numerical algorithms. In this context, the D2V17 set represents a third-order model, meaning that it can recover the momentum balance equation without errors. Physically, this allow the accurate computation of the viscous stress tensor.

The newly proposed method for solving the boundary system, combined with the use of high-order LB schemes, successfully predicted the incompressible flow in a 2D channel. The resulting velocity profile closely matches the analytical solution, and the development of the profile could be clearly analyzed.

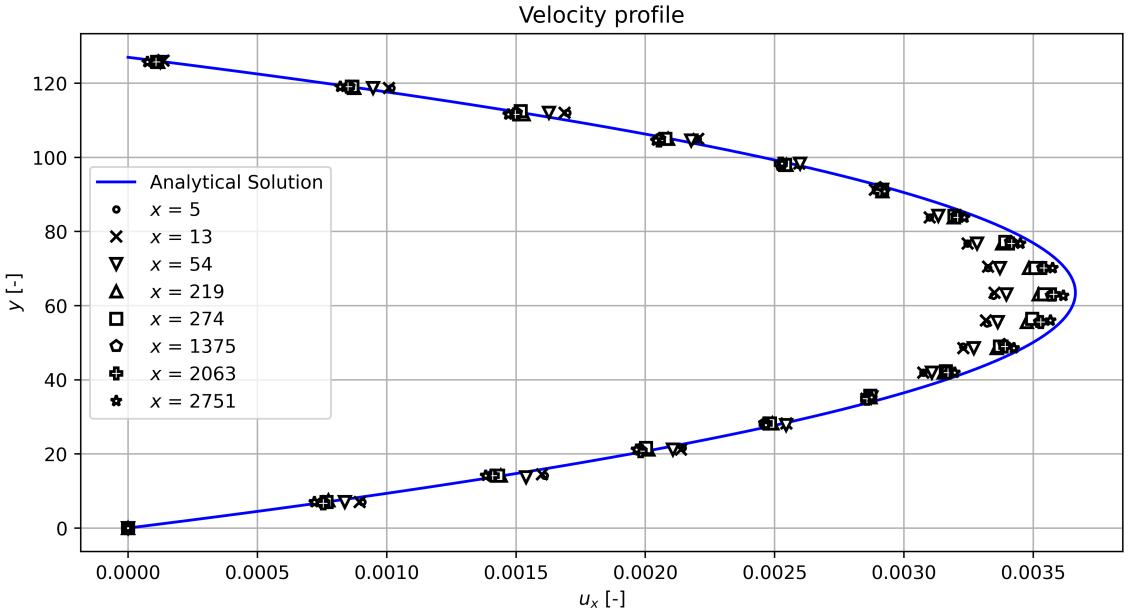


Figure 2. Numerical solution of velocity profile in different horizontal positions with $Re = 82$

Acknowledgements. The authors gratefully acknowledge the financial support provided by CAPES and CNPq.

Authorship statement. The authors hereby confirm that they are the sole liable persons responsible for the authorship of this work, and that all material that has been herein included as part of the present paper is either the property (and authorship) of the authors, or has the permission of the owners to be included here.

References

[1] L. A. Hegele, A. Scagliarini, M. Sbragaglia, K. K. Mattila, P. C. Philippi, D. F. Puleri, J. Gounley, and A. Randles. High-reynolds-number turbulent cavity flow using the lattice boltzmann method. *Physical Review E*, vol. 98, pp. 043302, 2018.
[2] R. L. Bazarin, P. C. Philippi, A. Randles, and L. A. Hegele. Moments-based method for boundary conditions in the lattice boltzmann framework: A comparative analysis for the lid driven cavity flow. *Computers and Fluids*, vol. 230, 2021.
[3] J. Latt, B. Chopard, O. Malaspinas, M. Deville, and A. Michler. Straight velocity boundaries in the lattice boltzmann method. *Physical Review E*, vol. 77, pp. 056703, 2008.
[4] L.-S. Luo, W. Liao, X. Chen, Y. Peng, and W. Zhang. Numerics of the lattice boltzmann method: Effects of collision models on the lattice boltzmann simulations. *Physical Review E*, vol. 83, pp. 056710, 2011.
[5] A. Hollis, I. Halliday, and C. M. Care. Enhanced, mass-conserving closure scheme for lattice boltzmann equation hydrodynamics. *Journal of Physics A: Mathematical and General*, vol. 39, pp. 10589–10601, 2006.
[6] Q. Zou and X. He. On pressure and velocity boundary conditions for the lattice boltzmann bgk model. *Physics of Fluids*, vol. 9, pp. 1591–1598, 1997.
[7] J. C. G. Verschaeve. Analysis of the lattice boltzmann bhatnagar-gross-krook no-slip boundary condition: Ways to improve accuracy and stability. *Physical Review E*, vol. 80, pp. 036703, 2009.
[8] O. Malaspinas, B. Chopard, and J. Latt. General regularized boundary condition for multi-speed lattice boltzmann models. *Computers and Fluids*, vol. 49, pp. 29–35, 2011.
[9] S. Mohammed and T. Reis. Using the lid-driven cavity flow to validate moment-based boundary conditions for the lattice boltzmann equation. *Archive of Mechanical Engineering*, vol. 64, pp. 57–74, 2017.
[10] P. L. Bhatnagar, E. P. Gross, and M. Krook. A model for collision processes in gases. i. small amplitude processes in charged and neutral one-component systems. *Physical Review*, vol. 94, 1954.
[11] K. K. Mattila, P. C. Philippi, and L. A. H. Junior. High-order regularization in lattice-boltzmann equations. *Physics of Fluids*, vol. 29, pp. 046103, 2017.
[12] O. Malaspinas. Increasing stability and accuracy of the lattice boltzmann scheme: recursivity and regularization. *arXiv:1505.06900v1 [physics.flu-dyn] 26 May 2015*, vol. , pp. 1–31, 2015.